Preparation and formulation of progesterone para-aminobenzoic acid co-crystals with improved dissolution and stability

European Journal of Pharmaceutics and Biopharmaceutics 196 (2024) 114202

Contents lists available at ScienceDirect

European Journal of Pharmaceutics and Biopharmaceutics

journal homepage: www.elsevier.com/locate/ejpb

Research paper

Preparation and formulation of progesterone *para*-aminobenzoic acid co-crystals with improved dissolution and stability

Thomas Hibbard, Kenneth Shankland, Hisham Al-Obaidi *

School of Pharmacy, University of Reading, Reading RG6 6AD, UK

ARTICLE INFO

Keywords:
Solubility
Co-crystals
Thermal analysis
Tablets
Progesterone

ABSTRACT

The crystal structure of a new Progesterone (PROG) co-crystal with *para*-aminobenzoic acid (PABA) showing enhanced solution properties is reported. PROG-PABA co-crystal was first identified though an *in silico* coformer screening process using the CSD Co-crystal deign function, then confirmed through a solution evaporation crystallisation experiment. The resulting co-crystal was characterized using single crystal X-ray diffraction, differential scanning calorimetry and Fourier-transform infrared spectroscopy. Liquid assisted grinding was selected as a suitable scale up method compared to spray drying and antisolvent methods due to minimal starting material phases in the final product. Following scale up, aqueous solubility, stability and dissolution measurements were carried out. PROG-PABA showed increased distinct aqueous solubility and dissolution compared to PROG starting material and was shown to be stable at 75 % relative humidity for 3 months. Tablets containing co-crystal were produced then compared to the Utrogestan® soft gel capsule formulation through a dissolution experiment. PROG-PABA tablets showed a substantial increase in dissolution over the course of the experiment with over 30× the amount of PROG dissolved at the 3-hour time point. This co-crystal shows positive implications for developing an improved oral PROG formulation.

1. Introduction

Progesterone (PROG) is an important female hormone that plays a key role in the menstrual cycle, pregnancy and embryogenesis [1,2]. Progesterone is a widely used therapeutic for treating various obstetric and gynaecological conditions, such as hormone replacement thefigrapy, contraception, and certain cancers. It is available in oral, vaginal, and transdermal forms, but the oral delivery method is preferred due to its ease of use, non-invasive nature, and overall suitability [1,2].

Oral administration of progesterone is complicated by low water solubility, an issue which must be addressed to ensure adequate absorption and clinical outcome. Current marketed formulations aim to address this issue by micronizing PROG then formulating as soft gel capsule (e.g. Utrogestan®) [3]. However, this is an imperfect solution since solubility remains relatively low for PROG causing limited bioavailability Soft gelatin capsules can be expensive to develop and may be vulnerable to heat, moisture, and microbial contamination. This can make them a less desirable option for certain applications in the field [4]. Alternative methods, such as tabletting and crystal engineering, have been explored to enhance the aqueous solubility of substances. These techniques have been implemented to increase the efficacy of pharmaceutical formulations and to improve their bioavailability.

Co-crystallisation is a promising crystal engineering formulation approach that has received much attention in recent years [5]. A co-crystal is a crystalline material composed of two or more different molecular entities, usually an active pharmaceutical ingredient (API) and a co-former, held together by non-covalent interactions [6]. The selection of a co-former has a substantial impact on the solubility, stability, and rate of dissolution of the co-crystal that is formed [7]. Co-crystallisation is favoured for APIs such as PROG over salt formation as it is a relatively neutral molecule without any readily ionisable functional groups. Co-crystals of PROG prepared through evaporation and liquid-assisted grinding experiments have been reported previously and these co-crystals show a variety of physical properties compared to PROG [8–11]. These studies have shown that certain PROG co-crystals have enhanced dissolution rates, leading to increased systemic exposure of the hormone [12]. The production of PROG co-crystals for pharmaceutical applications requires a continuous search for novel co-crystals to ensure the final solid form possesses the most beneficial physical and chemical properties for use in drug formulation.

* Corresponding author.
E-mail address: h.al-obaidi@reading.ac.uk (H. Al-Obaidi).

https://doi.org/10.1016/j.ejpb.2024.114202
Received 4 September 2023; Received in revised form 10 January 2024; Accepted 29 January 2024
Available online 2 February 2024

Solid dispersions are another approach to improve the dissolution kinetics and oral bioavailability of poorly water-soluble drugs such as PROG [13]. A solid dispersion is a formulation strategy in which the poorly soluble drug is dispersed in an inert carrier or matrix at a molecular level. The matrix may be composed of hydrophilic polymers, surfactants, or other suitable small molecules [14]. Converting PROG from its crystalline form to the amorphous form within these matrices can greatly enhance dissolution rates. This is due to the fact that amorphous drug forms tend to dissolve faster than their crystalline counterparts, as they are higher in energy and do not have a well-defined crystal structure. Moreover, the hydrophilicity of the matrix further improves the wetting properties of the drug, resulting in faster dissolution.

Both co-crystals and solid dispersions demonstrate the potential to address the unique challenges associated with oral administration of progesterone. The focus of previous research has been on the development of micronized PROG formulations with the aim to reduce particle size to enhance dissolution [14]. However, particle size reduction can be associated with altered rates of dissolution due to aggregation [15]. When developing formulations for PROG, it is reasonable to consider using co-crystals or solid dispersions-based formulations. However, it is important to have a comprehensive understanding of the interactions between PROG and the co-former or matrix, as well as their physicochemical stability. Careful characterization of the solid-state properties of any newly discovered API solid form is crucial since both crystalline and amorphous forms can be produced through similar methods. Therefore, it is essential to accurately identify the solid-state properties to ensure the quality and efficacy of the final product [14].

The present study outlines a screening process employed to identify a novel co-crystal of PROG and *para*-aminobenzoic acid (PABA). The newly discovered co-crystal was subjected to comprehensive characterization through X-ray diffraction, thermal, and spectroscopy analysis. The development of a reliable scale-up method for the newly discovered PROG-PABA co-crystal was also explored through antisolvent, spray drying, and liquid-assisted grinding techniques. Following scale-up, the stability, aqueous solubility, and in vitro dissolution were assessed, including a comparison of dissolution between a co-crystal tablet formulation and the marketed PROG formulation of Utrogestan®. The co-crystal tablet formulation was also compared to existing oral PROG formulations, and to the best of our knowledge, this is the first report on this co-crystal being formulated into a tablet for comparative analysis.

2. Material and methods

2.1. Materials

Progesterone (PROG), *para*-aminobenzoic acid (PABA), α-lactose monohydrate, Polyplasdone™ XL (crospovidone), magnesium stearate and sodium lauryl sulphate were obtained from Sigma-Aldrich (Dorset, UK). HPLC water, acetonitrile, ethanol and propan-2-ol were obtained from Fisher-Scientific Limited (Leicestershire, UK). Utrogestan® capsules (UTRO) were used as a comparison for dissolution studies. All chemicals were used as received.

2.2. Preparation of PROG co-crystal and formulations

2.2.1. Co-crystal screening

An *in silico* co-crystal screen was performed using the "co-crystal design" function of Mercury which screens an API molecule against a bank of coformers based on molecular compatibility [16]. The tool analyses reported crystal structures of molecules and compares key molecule properties which are likely to influence the formation of a co-crystal. Following the generation of 32 matches, 6 coformers were chosen for crystallisation experiments to cover a range of coformer molecular characteristics. These were: *para*-aminobenzoic acid, caffeine, hippuric acid, methylparaben, pimelic acid and tartaric acid (Fig. 1).

PROG and coformers were dissolved in separate vials to a concentration of 10 mg/mL using propan-2-ol. PROG and a coformer solution containing an equimolar quantity of coformer were then filtered and pipetted into a single well of a 24-well plate. By creating stock solutions of PROG and conformers, equimolar solvent systems could be created and measured out rapidly using volume measurement rather than weighing microgram amounts. The above process was repeated with the each coformer and then the plate was sealed, and the solutions left to crystalise in a temperature-controlled incubator over 3 days. Resulting crystals were isolated and analysed through single crystal X-ray diffraction.

2.2.2. Liquid assisted grinding experiments (LAG)

Equimolar quantities of PROG and PABA were milled using a Retsch MM 500 nano mill with the addition of 20 μL of ethanol [17]. All experiments were performed for 30 mins at 25 Hz with 2.5 mm stainless steel ball bearings in a 1:20 mass ratio to the starting materials. The LAG powder was transferred to a vial and stored in a desiccator.

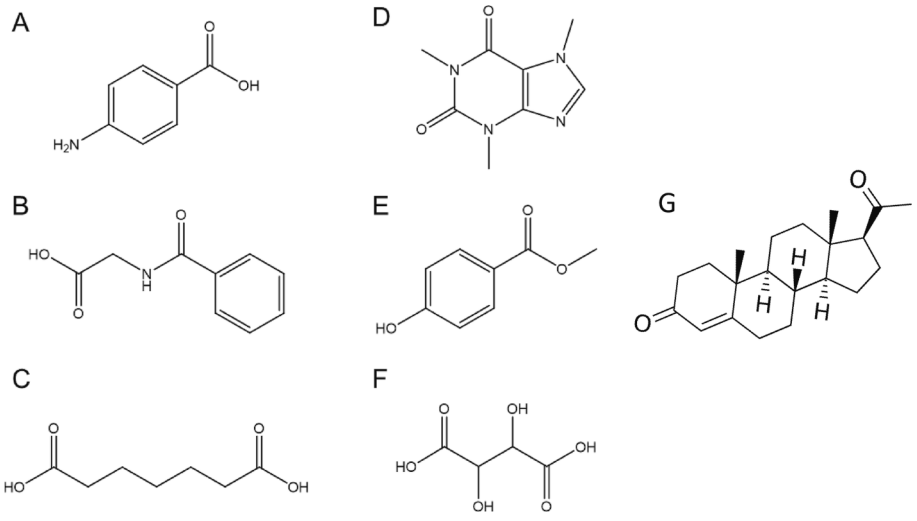

Fig. 1. Chemical structures of molecules selected for experimental coformer screening. (A) *para*-aminobenzoic acid, (B) hippuric acid, (C) pimelic acid, (D) caffeine, (E) methylparaben, (F) tartaric acid, (G) progesterone.

2.2.3. Antisolvent experiments (AS)

Equimolar quantities of PROG and PABA were added to a vial and dissolved in the minimal volume of propan-2-ol to form a saturated solution. This solution was then pumped dropwise into an antisolvent solution of 200 mL ultrapure water at 2 mL/min. Any precipitate formed was isolated using vacuum filtration and dried in an incubator at 25 °C, transferred to a vial then stored in a desiccator.

2.2.4. Spray drying experiments (SD)

Spray drying experiments were performed using a B-290 spray dryer (Büchi, Laboretechnik AG Switzerland) which used a nitrogen atomising gas and nitrogen drying atmosphere operated in a closed loop mode. The aspirator was set to 100 %, the inlet temperature at 120 °C and experiments were started when the outlet temperature stabilised at 60 °C. A two-fluid nozzle with nozzle diameter 0.5 mm was used and the feedstock was pumped at 5 mL/min. The feedstock was composed of PROG and PABA dissolved in propan-2-ol at a 1:1 M ratio to a concentration of 2 % w/v. Spray dried powder was transferred to a vial and stored in a desiccator.

2.2.5. Tablet formulation

PROG co-crystal tablets were formulated with the excipients detailed in Table 1 using the PROG-PABA co-crystal produced through liquid assisted grinding (Section 2.2.2).

LAG co-crystal powder was blended with PolyPlasdone XL and α-Lactose monohydrate using a sheer mixer. Then, magnesium stearate was added, and the powder tumble mixed for 2 mins to coat with lubricant.

250 mg tablets were produced using a manual fill, direct compression method with a 0.9 cm diameter round punch. The tabletting machine was set to a compression depth of 10 mm and manually operated. 10 mm was selected as a suitable compression depth during method development as it gave a tablet of an appropriate thickness and in an agreed hardness range of 8–10 N. Since harness is not a standard pharmacopeia measurement the range was chosen as acceptable within the specification of the tabletting machine being used. All tablets were individually weighed and only those weighing 250 mg ± 5 % were accepted for further testing.

2.3. Physicochemical analysis

2.3.1. Single crystal X-ray diffraction (SC-XRD)

Single crystals showing birefringence under polarised light were selected for analysis, isolated in Paratone-N oil and mounted onto a crystal analysis loop. Diffraction data at 100 K were collected using a Rigaku Synergy diffractometer equipped with a Cu microsource, a HyPix detector and an Oxford Cryosystems Cryostream device. Crystal structures were solved using ShelXT [18] and refined using ShelXL [19] (using the Olex2 [20] program) and crosschecked with the Cambridge Structural Database (CSD) database [21], then rendered using Mercury [22].

2.3.2. Powder X-ray diffraction (PXRD)

Transmission capillary PXRD data were collected using a Brucker D8 Advance diffractometer (Billerica, MA, USA) equipped with a monochromatic CuKα_1 source. Samples were packed into a 0.7 mm borosilicate glass capillary then scanned in the range 4°–45° 2θ using step size 0.0171° with a count time of 1.4 s per step. Data for the starting materials were also collected using the same settings to be used as a reference. PXRD data for the tablet surface was collected using a Brucker D8 Advance diffractometer operating in a reflection geometry using the same settings as the transmission data collection. Phase Rietveld fit was performed using TOPAS compared to experimental SC-XRD co-crystal unit cell parameters and those from Cambridge Structural Database (CSD) structures: PROGST10 and AMBNAC06.

Table 1
Tablet composition.

Component	Tablet Weight (250 mg)
Progesterone (as co-crystal)	20 %
Disintegrant (PolyPlasdone XL)	3 %
Lubricant (magnesium stearate)	1 %
Filler (α-Lactose monohydrate)	to 100 %

2.3.3. Fourier-transform infrared spectroscopy (FTIR)

FTIR spectra were collected using a Perkin-Elmer 100 FTIR Spectrometer equipped with a diamond attenuated total reflectance (ATR) accessory (Shelton, CT, USA). Transmission was recorded from an average of 16 scans over the range 650–4000 cm^{-1} with a resolution of 4 cm^{-1}.

2.3.4. Differential scanning calorimetry (DSC)

Thermal properties of samples were analysed using DSC with samples hermetically sealed into aluminium pans with pierced lids to allow for any pressure release. All samples were heated to 190 °C at 10 °C/min in a N_2 atmosphere using a TA Q2000 DSC instrument (New Castle, DE USA). Results were analysed using TA Universal Analysis to identify thermal events.

2.3.5. Scanning electron microscopy (SEM)

Images of samples were obtained using a Quanta 600F scanning electron microscope (Hillsboro, ORE, USA) under high vacuum. Samples were attached to carbon tabs, mounted on aluminium pins, then sputter-coated with gold for 3 min at 30 mA (Emitech K550).

2.4. Physical property analysis

2.4.1. Stability

LAG co-crystal powder was weighed into vials and stored in a sealed container at 37 °C and 75 % relative humidity. 75 % relative humidity was generated by adding a reservoir containing a saturated NaCl solution to the sealed container separate from the powders. Humidity was verified using a humidity testing meter.

2.4.2. UV-HPLC

PROG separation was achieved with ACE 3 C18 column (75 × 4.6 mm, 3 μm) and gradient elution with water:acetonitrile mobile phase. The UV detector was set to 245 nm for PROG and 290 nm corresponding to reported lambda max values. A linear calibration curve was generated ($r^2 > 0.99$) from a stock solution of PROG in 50:50 acetonitrile:water over a range of 0.1 mg/mL to 200 mg/mL.

2.4.3. In-vitro solubility analysis

The solubility of LAG co-crystal and PROG were assessed in ultrapure water over a period of 48 h at 20 °C (±1 °C) in triplicate. Excess solid was added to 1 mL of UP-H_2O and mixed on a mechanical mixer with temperature probe to monitor temperature. At 72 h, samples were centrifuged at 13,000 rpm for 5 mins then the supernatant was collected, diluted, and PROG and PABA concentrations were determined using HPLC.

2.4.4. Dissolution studies

Dissolution experiments comparing LAG co-crystal to PROG starting material and then co-crystal tablet to UTRO formulation were performed using the following method. All experiments were performed using a Copley Scientific DIS 8000 instrument equipped with paddle dissolution apparatus. Experiments were run at 37.5 °C (±0.5 °C) with stirring at 50 rpm over 2 h in 900 mL of degassed ultrapure water. Samples were removed at time intervals of 5, 15, 30, 60 and 120 mins, filtered using a 0.22 μm syringe filter (Ministart®) and PROG concentration determined using the HPLC method outlined in Section 2.4.2. For co-crystal and

PROG powder dissolution experiment, a size 0 gelatine capsule was filled with powder equivalent to 100 mg PROG placed in a stainless-steel capsule sinker. For co-crystal tablet and UTRO experiments, tablets equivalent to 100 mg of PROG and a Utrogestan® 100 mg capsule were used. A capsule sinker was used for the UTRO formulation and the experiment was performed in 900 mL of 0.1 % w/v sodium lauryl sulphate (SLS) solution. Residual UTRO capsule and co-crystal tablet were isolated and analysed using FTIR.

3. Results

3.1. Co-crystal screening and characterisation

3.1.1. Single crystal X-ray diffraction

All co-crystal crystallisation screening experiments yielded crystals suitable for SC-XRD analysis. SC-XRD solid phase analysis showed that PROG had formed a unique solid phase with PABA yet PROG and the other coformers had crystalised in separate solid phases. Although co-crystals did not form with these other coformers, successful co-crystal generation may occur provided the correct solvent systems and crystallisation conditions are utilised.

CSD searching showed that the PROG-PABA co-crystal was a novel crystal structure and was selected for further experimentation. Table 2 summarises the crystal information of the PROG-PABA co-crystal.

PROG-PABA crystallises in space group $P2_12_12_1$ with two PROG and two PABA molecules in the asymmetric unit (Fig. 2). The carboxylic acid groups of the PABA molecules pair up in an $R_2^2(8)$ motif. The amino group of one PABA molecule forms a $C_2^1(4)$ motif with two symmetry-related PROG molecules, H1A-N1-H1B…O1…H1A, whilst the amino group of the other PABA molecule links with O2 of the aforementioned PROG molecule (N2-H2A…O2) and O4 of the other PROG molecule (N2-H2B…O4) which is not H-bonded to any other molecules in the structure.

Changes to the nature of intermolecular bonding in the carbonyl and amine regions is also seen when comparing the FTIR data of starting materials and co-crystal (Figs. S1 and S2). At the amine region of absorption, corresponding with the N—H stretch (i.e. 3400–3250 cm^{-1}), there is a "blue-shift" in peak positioning corresponding to a shortening of the hydrogen bond for PABA when bonding with PROG rather than itself.

Similarly, in the carbonyl region of absorption, corresponding to C═O stretching (i.e. 1760–1690 cm^{-1}), the blue-shift associated with PROG C═O bond from ~1695 cm^{-1} to ~1690 cm^{-1} is observed. This change to a higher energy frequency is expected since this functional group begins to participate in hydrogen bonding, rather than short contact interactions, following formation of a co-crystal, since PROG does not possess any hydrogen bond donor groups.

This blue-shifting in functional groups is in line with previously reported co-crystals of PROG and is indicative of the formation of strong intermolecular hydrogen bonds [8,10].

DSC was used to analyse the thermal properties of the PROG-PABA co-crystal and showed a single sharp endothermic event with onset temperature of 153.98 °C (Fig. 3). This corresponds to the melting point of the co-crystal and is situated between the melting points of PROG and PABA at 129.72 °C and 188.22 °C respectively. The melting point increase compared to the PROG starting material is in line with the formation of intermolecular hydrogen bonds within the co-crystal structure.

Table 2
SC-XRD data for PROG-PABA co-crystal.

Summary	
Identification code	PROG-PABA
Empirical formula	$C_{28}H_{37}NO_4$
Formula weight	451.58
Temperature/K	99.99(10)
Crystal system	orthorhombic
Space group	$P2_12_12_1$
a/Å	7.54410(10)
b/Å	12.90940(10)
c/Å	49.8923(5)
α/°	90
β/°	90
γ/°	90
Volume/Å3	4859.00(9)
Z	8
ρ_{calc}g/cm^3	1.235
μ/mm^{-1}	0.647
F(000)	1952.0
Crystal size/mm^3	0.19 × 0.04 × 0.03
Radiation	Cu Kα (λ = 1.54184)
2Θ range for data collection/°	7.074 to 153.068
Index ranges	$-9 \le h \le 8$, $-16 \le k \le 15$, $-61 \le l \le 60$
Reflections collected	45,225
Independent reflections	9768 [R_{int} = 0.0430, R_{sigma} = 0.0312]
Data/restraints/parameters	9768/0/625
Goodness-of-fit on F^2	1.039
Final R indexes [I ≥ 2σ (I)]	R_1 = 0.0331, wR_2 = 0.0839
Final R indexes [all data]	R_1 = 0.0377, wR_2 = 0.0862
Largest diff. peak/hole/e $Å^{-3}$	0.17/−0.18
Flack parameter	−0.04(6)

3.2. Co-crystal scale up characterisation

Spray drying, antisolvent and liquid assisted grinding methods were investigated for scale up of the PROG-PABA co-crystal as described in Sections 2.2.2–2.2.4. Successful co-crystal preparation was determined through Powder X-ray Diffraction (PXRD) compared to a simulated PXRD pattern from the PROG-PABA crystal structure (Mercury).

PXRD analysis of LAG, AS and SD product indicated co-crystal formation for all three methods. Each product contains diffraction peaks which correspond well with the simulated powder pattern generated from the PROG-PABA SC-XRD data (Fig. 4, Fig. S3). This is most clearly seen with the generation of new diffraction peaks at ~7, ~9.7 and ~12.2 °2θ and the elimination of starting material reference peaks at ~9.5 and 12.8 °2θ for PROG and ~9.52 and ~14.79 °2θ for PABA, although some starting material peaks still remain. SD and AS methods show larger crystallite size compared to the LAG method as seen by larger FWHM values i.e. peak at ~7 °2θ, LAG = 0.067°, AS = 0.084°, SD = 0.117° and they also show larger proportion of non co-crystal diffraction peaks. There are also additional peaks present in the AS and SD formulations which are not accounted for by the starting materials or co-crystal. These peaks, e.g. at ~13.7 °2θ and ~14.7 °2θ and ~20 °2θ are likely to be due to the presence of additional phase formed alongside the co-crystal. We conclude that this phase can be attributed to the Form II polymorph of PROG which is known to be favoured following rapid precipitation [23] or the formation of solvates. To further quantify these impurities, three-phase Reitweld fit of the single-crystal co-crystal structure, PROG and PABA starting materials compared to the LAG sample and AS PXRD data was carried out. For the LAG sample, this yielded a R_{wp} of 3.9 with no unfitted features showing a phase composition of >90 % co-cocrystal with the remaining amount explained by starting material phases (Fig. S4a and S4b) as is common with mechanochemical activation of co-crystals [15]. Further liquid-assisted grinding method optimisation or introduction of a purification step will be required to increase the % co-crystal in future work. The AS sample refinement showed a Rwp of 9.5 which included several unfitted features confirming the presence of other phases in the product and a lower purity than the LAG sample (Fig. S4c), Nevertheless, the co-crystal was still the predominant phase in the sample. Reitweld refinement was unable to be completed for the SD sample due to poor quality diffraction data and several strong peaks whose presence cannot be explained by the presence of starting materials.

Co-crystals prepared through LAG, AS and SD methods were also viewed using SEM (Fig. 5). All preparation methods show a similar

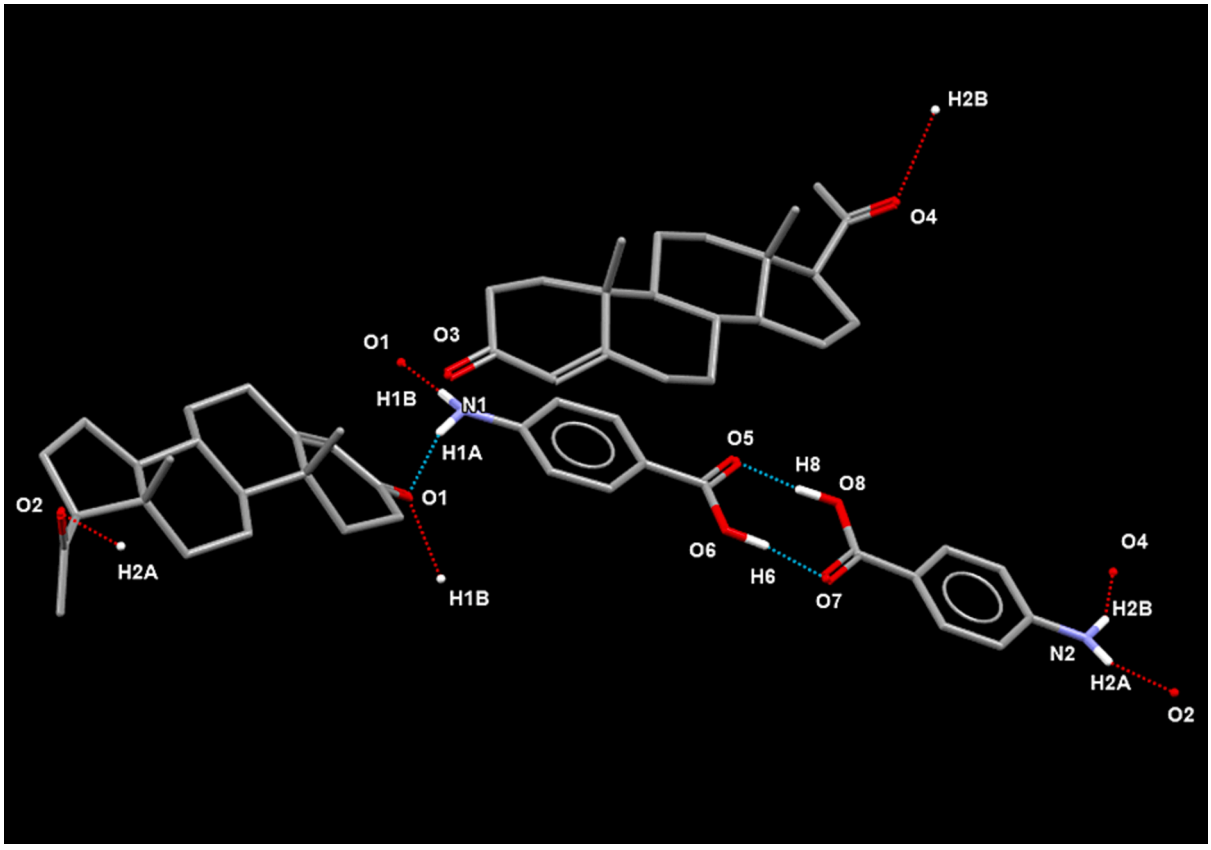

Fig. 2. A Mercury diagram for the PROG-PABA asymmetric unit, showing hydrogen bonding between key bonding functional groups (dashed lines).

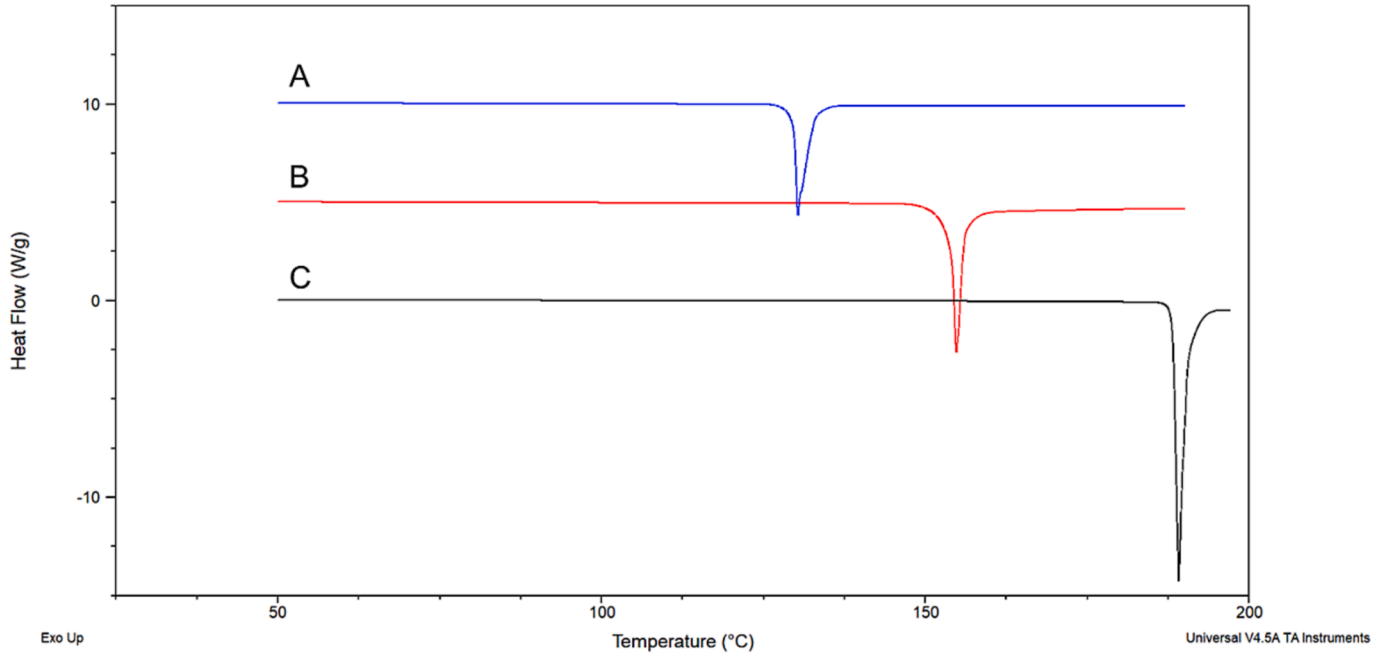

Fig. 3. DSC Data for (A) progesterone reference (blue), (B) PROG-PABA co-crystal (red), (C) *para*-aminobenzoic acid reference (black). (For interpretation of the references to colour in this figure legend, the reader is referred to the web version of this article.)

particle size although there are clear differences in the morphology between the LAG and solvent based methods. AS and SD methods show clearly defined crystals with needle like morphology as well as agglomerate like particles in the sample. The LAG co-crystal appears to be more uniform in morphology with the absence of needle like crystals.

DSC measurements were taken for the LAG co-crystal to investigate the potential formation of an amorphous phase during the high energy liquid assisted grinding process. The thermal analysis showed a single strong endothermic thermal event at 154 °C which was attributed to the melting point of PROG-PABA cocrystal (Fig. S5). In the absence of

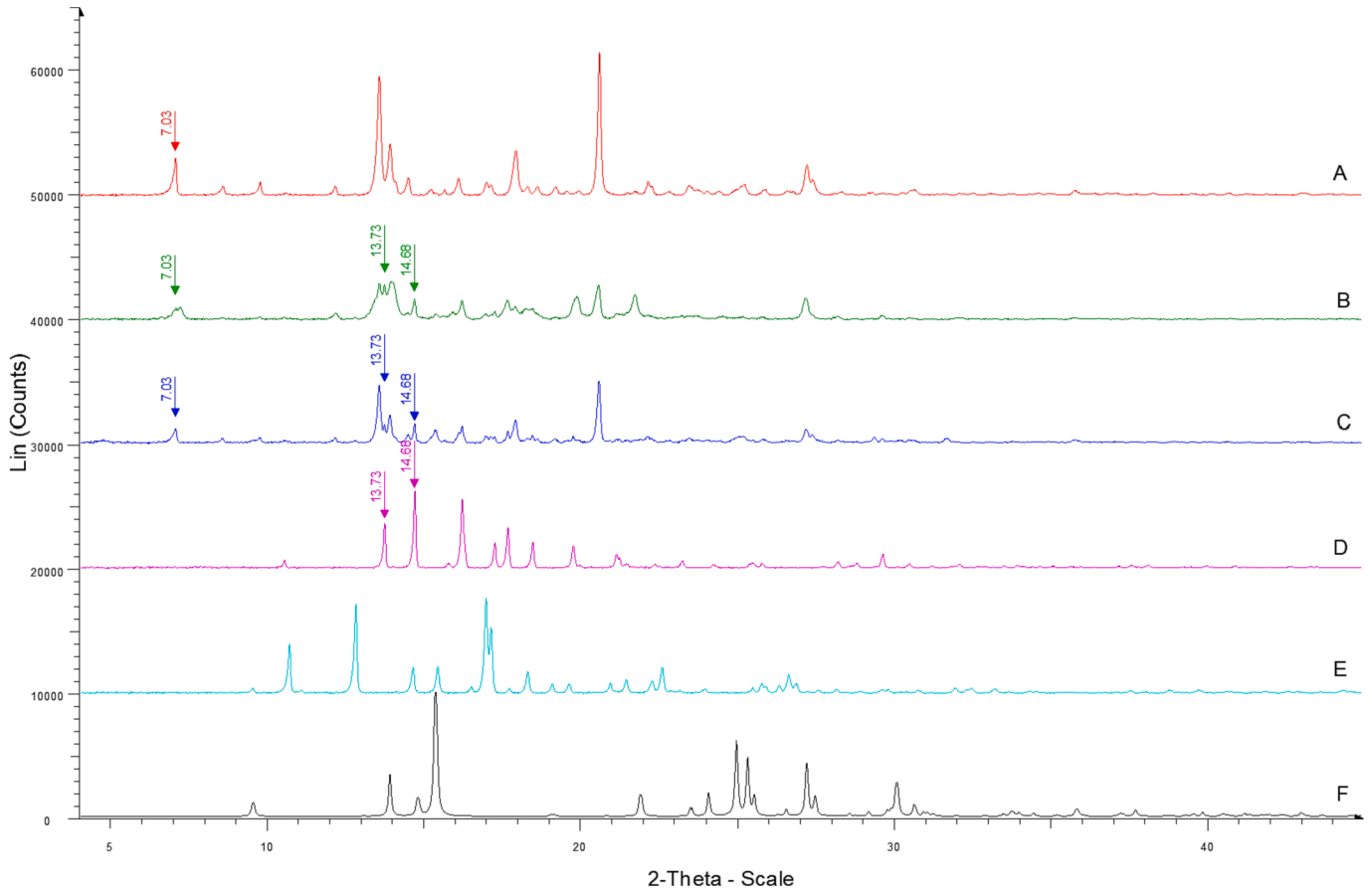

Fig. 4. PXRD data showing (A) PROG-PABA liquid assisted grinding (Red), (B) PROG-PABA spray dried (Green), (C) PROG-PABA antisolvent (Blue), (D) PROG Form II polymorph reference (Pink), (E) PROG Form I polymorph reference, (F) PABA Reference. Note PROG Form II (D) peaks at 13.73° 2θ and 14.66° 2θ in antisolvent product (B) and spray dried (C) products. (For interpretation of the references to colour in this figure legend, the reader is referred to the web version of this article.)

additional thermal events, particularly a glass transition step, it was concluded that a significant amorphous phase had not been produced during scale up manufacture. There is also little indication of thermal events associated with excess starting materials shown in the Reitweld refinement, as such, these phases were considered insignificant to bulk material physicochemical properties.

Due to minimal residual starting material, absence of new additional phases and relatively uniform particle size and morphology, liquid assisted grinding was selected as a suitable scaleup method for preparing this co-crystal and used for further experiments.

3.3. Physical property analysis

3.3.1. In vitro stability study

Following preparation through liquid assisted grinding, PXRD and FTIR reference spectra for LAG PROG-PABA were collected, then the co-crystal was stored in a high relative humidity environment for three months. PXRD data following three months shows no apparent difference in the diffraction pattern for PROG-PABA, seen through identical peak positioning and the absence of any additional diffraction peaks (Fig. 6). If the co-crystal form had changed or degraded over the course of the experiment, clear changes to the crystal structure would have been seen by the X-ray diffraction pattern.

FTIR data confirms there was no structural change during the experiment through identical functional group peak positionings which are indicative of the same molecular bonding environment (Fig. S6). Also, in the absence of any additional absorption at ~3500 cm^{-1}, FTIR confirms that there has been no absorption of water into the sample from the high humidity atmosphere. Therefore PROG-PABA was seen as a stable crystalline compound through testing at accelerated storage conditions.

3.3.2. LAG powder solubility and dissolution studies

The data showed no significant difference between the concentration of PROG in aqueous solution at 48 hrs when comparing PROG and PROG-PABA co-crystal (Fig. 7). PXRD analysis shows the residual solid phases at 48hrs to be PROG Form I and PROG-PABA exclusively (Fig. S7). Therefore, these solubility values correspond to PROG Form I and PROG-PABA in equilibrium with water respectively.

The mean solubility value for PROG-PABA is higher than PROG although there was considerably higher variation around the mean leading to no significant difference. Some co-crystal repeats show double the concentration of PROG in solution which suggests that the co-crystal may be able to initiate a higher solubility which is kinetic in nature and works towards equilibrium at 48 hrs. Further experimentation detailing the extent and duration of a higher kinetic solubility is required through concentration analysis at time points during the experiment.

Comparing dissolution of PROG-PABA powder to PROG Form I starting material shows a clear increase in dissolution for the co-crystal compared to pure PROG, as shown in Fig. 8. This is most clearly seen within the first 30 mins of the experiment, where, by the 5 min time point, PROG-PABA shows ~10 % dissolution compared to ~1 % dissolution for PROG. This difference increases to 20 % by the 15 min time point where PROG-PABA has reached ~30 % dissolution. However, both experiments appear to have plateaued by the 30 min time point at ~15 % and ~35 % dissolution for PROG and PROG-PABA respectively which continues until the end of the experiment. The plateau signifies

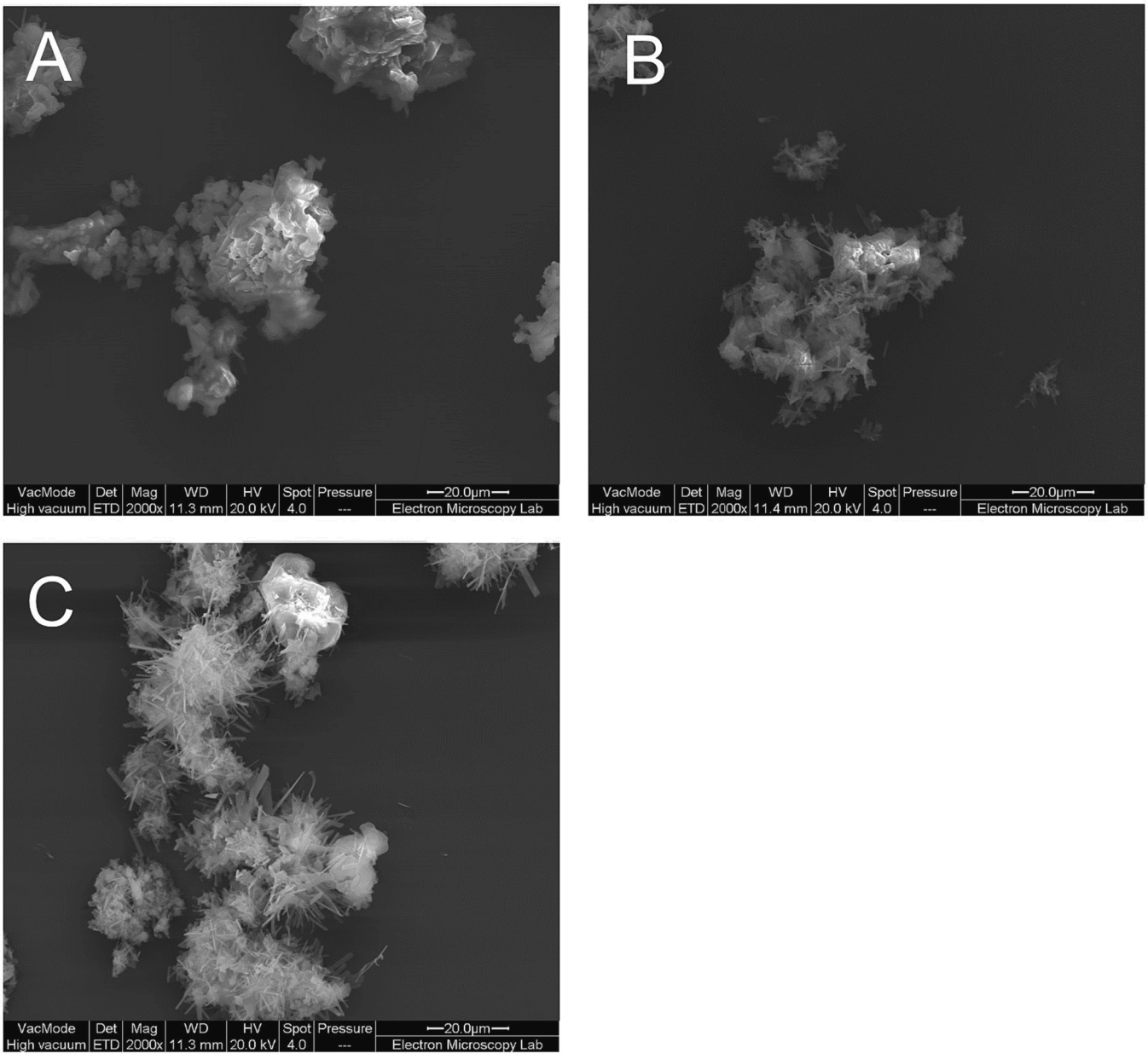

Fig. 5. SEM images comparing (A) PROG-PABA LAG, (B) PROG-PABA SD, (C) PROG-PABA AS.

that the concentration of PROG in the solution has reached its saturation solubility, a state where the dissolution process enters a dynamic equilibrium. In this state, the rate of PROG dissolving into the solution is precisely balanced by the rate of PROG precipitating out of the solution. This equilibrium is a typical occurrence in dissolution studies, especially in systems where the solute exhibits limited solubility in the dissolution medium. The higher dissolution percentage observed for the PROG-PABA co-crystal, compared to pure PROG, reflects the enhanced solubility afforded by the co-crystal structure, which facilitates better solubilization in the dissolution medium. However, despite this improved solubility, the co-crystal also reaches its saturation point under non-sink conditions, beyond which no further dissolution occurs, resulting in the plateau. Initially, the dissolution rate is influenced by kinetic solubility, which can be higher than the equilibrium solubility, leading to rapid dissolution in the early stages. As the experiment progresses and the system transitions towards equilibrium solubility, the effects of non-sink conditions become more pronounced, culminating in the plateau. The experimental conditions, including the use of degassed ultrapure water and specific temperature and stirring settings, also contribute to determining the solubility limit of PROG in the solution under these non-sink conditions. These controlled conditions were consistent across all experiments, providing a reliable environment to assess the dissolution behavior of both PROG and PROG-PABA.

3.3.3. PROG-PABA tablet formation

Tablets were produced using a direct compression method described in Section 2.2.5 and tablets of the required mass and of a suitable hardness were selected for further testing [24,25]. Following tablet formation, the tablet surface was analysed via PXRD using a flat plate function in reflectance mode (Fig. S8). PROG-PABA can be identified on the surface of the tablet although the peaks are much lower in intensity than those of α-Lactose monohydrate. Identification of co-crystal and excipient peaks on the surface of the tablet highlights the generation of a good physical mix between co-crystal and excipients during the formulation process. Identification of the co-crystal also points to the stability of PROG-PABA through the direct compression tabletting

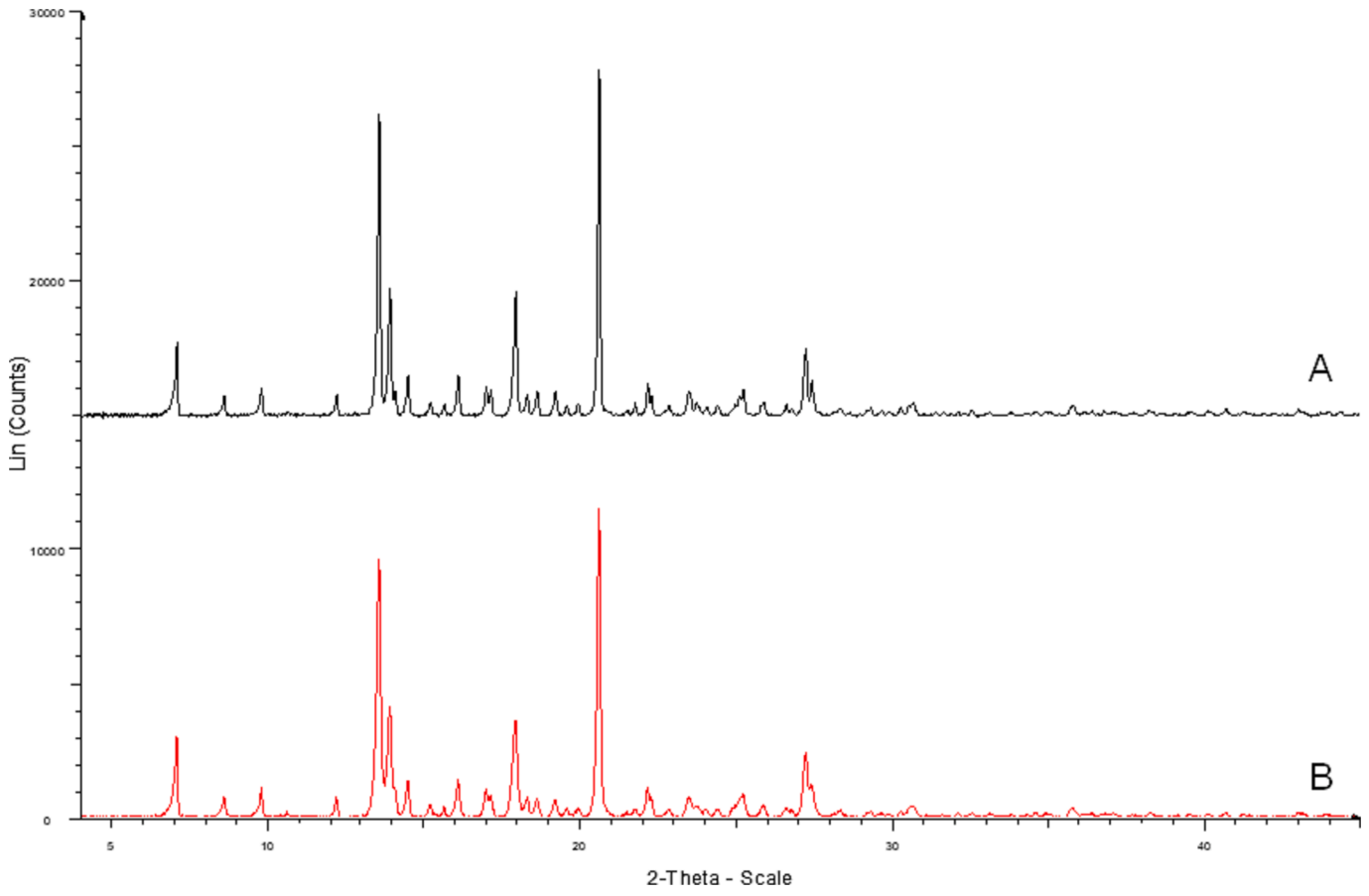

Fig. 6. PXRD data for LAG PROG-PABA (A) after humidity study for 3 months at 37.5 °C and 75 % relative humidity (black), (B) before humidity study (red). (For interpretation of the references to colour in this figure legend, the reader is referred to the web version of this article.)

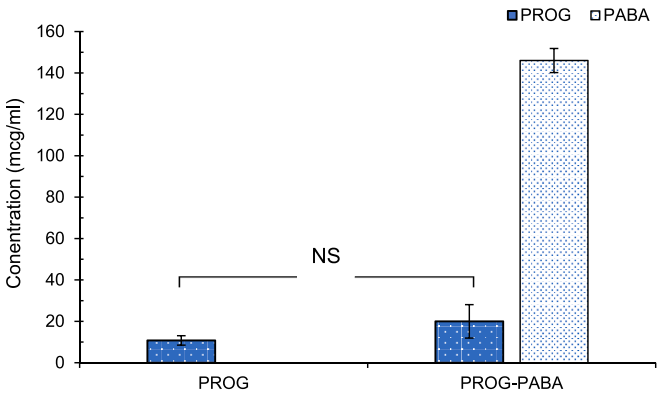

Fig. 7. Aqueous solubility data for PROG and PROG-PABA co-crystal at 48 h. Data expressed as a mean with error bars showing standard deviation (n = 3), ANOVA, $p > 0.05$.

process suggesting that this is a suitable formulation method for oral delivery.

3.3.4. *PROG-PABA tablet dissolution*

Dissolution experiments comparing the PROG-PABA tablet with UTRO formulation were performed in 0.1 % SLS media as per the precedent for using SLS in literature [26,27]. There is a clear increase in dissolution of PROG from the tablet formulation compared to the soft capsule formulation as shown in Fig. 9. After 5 mins, PROG dissolution of 17.5 % was observed from the tablet formulation compared to 0.5 % in the soft capsule. This increase in dissolution continues throughout the experiment where at the 3-hour time point, 46 % and 1.7 % dissolution were observed for the tablet and soft capsule respectively. This is an almost 30× increase in the amount of PROG dissolved compared to a current marketed formulation. To validate these findings, the residual solid phases from the dissolution experiment were filtered from the dissolution media and their composition analysed. FTIR analysis confirmed the presence of PROG for solid residues from both tablet and soft-gelatine capsule dissolution experiments (Fig. S9). This indicates that the low % dissolution seen for UTRO was due to poor solution properties rather than sampling error during the dissolution experiment. With respect to the tablet formulation, presence of PROG rather than PROG-PABA in the dissolution residue suggests that PROG has dissolved then precipitated out of solution during the course of the experiment. This fits with the understood "spring and parachute" model of supersaturation which has been suggested to described co-crystal solution properties [28].

The PROG-PABA tablet also shows an increase in dissolution compared to the PROG-PABA powder filled capsule. This is likely to be due to two main factors, firstly, it points to the utility of the tablet formulation for encouraging disintegration and therefore promoting better dissolving at the start of the experiment. This is seen by an increase of ~10 % in dissolution between powder and tablet formulations at the 5 min time point. The rapid release of PROG into solution from the tablet could mean that the tablets produced disintegrated rapidly. The study did not involve assessment of disintegration times and as such further development of the tabletting procedure through varying compression depth and punch size to increase tablet harness may be required.

Secondly, the addition of 0.1 % surfactant to the dissolution media will facilitate a higher amount of PROG in solution as seen by comparing

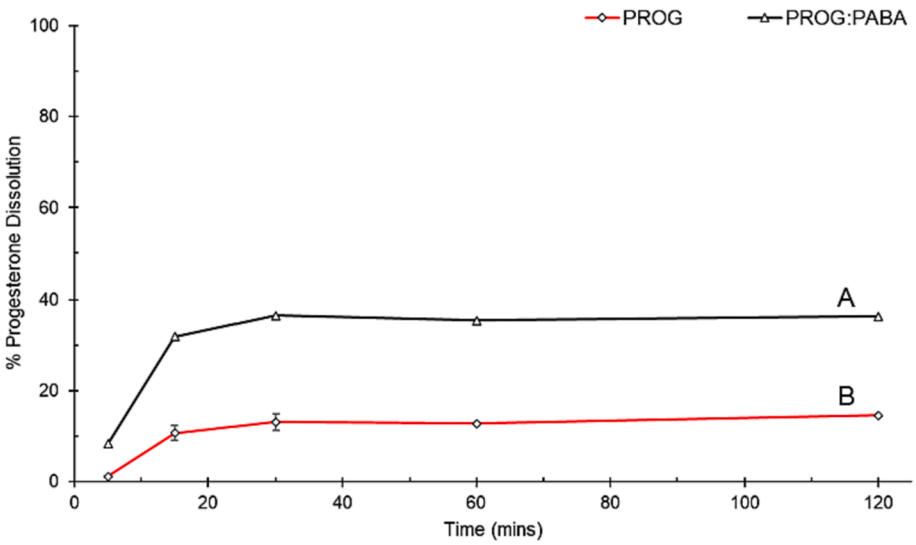

Fig. 8. Dissolution data for powder dissolution experiment. (A) PROG-PABA LAG powder (black) and PROG starting material (red). Data expressed as a mean with error bars showing standard deviation (n = 3). (For interpretation of the references to colour in this figure legend, the reader is referred to the web version of this article.)

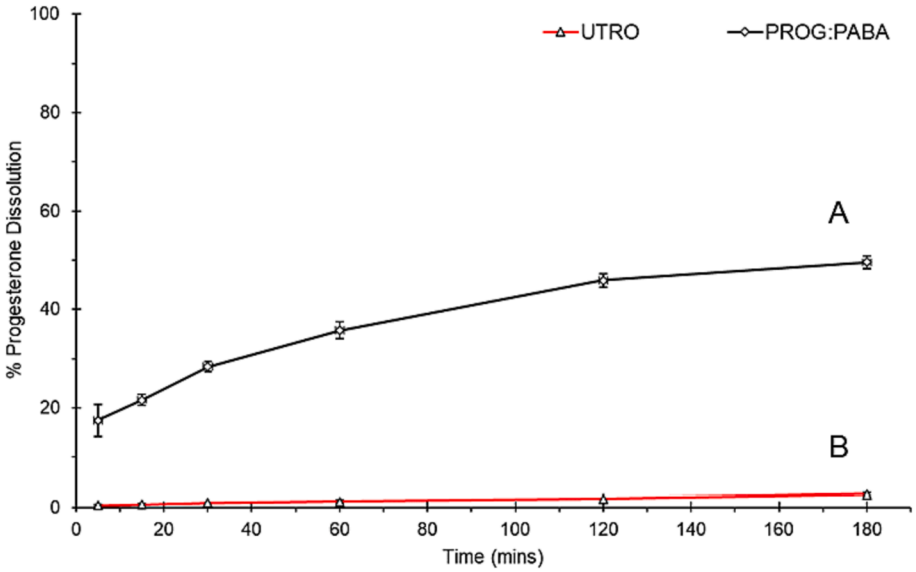

Fig. 9. PROG-PABA tablet vs Utrogestan® dissolution experiment. Data expressed as a mean with error bars showing standard deviation (n = 3).

the % dissolution at the 2-hour mark i.e. ~35 % dissolution compared to ~45 % dissolution. The tablet formulation also seems to be continuing to trend up wards at the end of the experiment compared to powder dissolution which has plateaued. In general, these experiments show the benefits of co-crystallisation and tablet formulation on the dissolution of PROG.

4. Discussion

The development and characterization of the PROG-PABA co-crystal in this study represent a significant advancement in pharmaceutical formulation, particularly in enhancing drug solubility and stability. The novelty of this work lies in the successful creation of a new solid phase, as confirmed by Single Crystal X-ray Diffraction (SC-XRD) and Cambridge Structural Database (CSD) searching. This achievement is notable because co-crystals, as a means to modify drug properties, have been increasingly recognized in recent pharmaceutical research, yet the development of novel co-crystals with distinct and improved properties remains a challenging effort.

The use of Fourier Transform Infrared Spectroscopy (FTIR) to observe changes in the carbonyl and amine regions of PROG-PABA indicates a unique interaction between PROG and PABA, enhancing the co-crystal's stability and solubility. This finding aligns with the growing body of research suggesting that co-crystals can significantly alter the physical properties of drugs, leading to improved therapeutic efficacy and stability. In terms of scale-up characterization, the study explores various methods like spray drying, antisolvent, and liquid-assisted grinding, demonstrating a comprehensive approach to pharmaceutical manufacturing. The Powder X-ray Diffraction (PXRD) analysis confirms the reproducibility of the co-crystal's structure in scaled-up batches, a crucial factor for commercial pharmaceutical production. This aspect of the study is particularly relevant given the current focus in pharmaceutical research on ensuring the scalability of novel drug formulations.

The physical property analysis, including Scanning Electron Microscopy (SEM) and Differential Scanning Calorimetry (DSC), provides valuable insights into the morphological and thermal properties of the

co-crystals. The SEM analysis, which reveals differences in morphology between co-crystals produced by different methods, contributes to our understanding of how preparation techniques can influence the final product's properties. The DSC results, indicating the absence of significant amorphous phases, further highlight the method's effectiveness in preserving the crystalline structure. The in vitro stability study of the co-crystal under high humidity conditions adds another layer of novelty to the research. The stability of pharmaceutical co-crystals under varying environmental conditions is a critical area of study, and the findings here suggest that PROG-PABA is a robust cocrystal suitable for long-term pharmaceutical applications. This aspect of the research is particularly important when considering the challenges associated with the stability of many pharmaceutical cocrystals.

The PROG-PABA co-crystal exhibited a significant increase in dissolution rate compared to pure PROG, with approximately 10 % dissolution observed within the first 5 min for the co-crystal, in contrast to just 1 % for PROG. This trend continued, reaching around 30 % dissolution at the 15-minute mark for the co-crystal, compared to 20 % for PROG. Such an improvement in dissolution rate is indicative of the co-crystal's potential for enhanced drug delivery efficiency. Additionally, the SEM analysis across various manufacturing methods (spray drying, antisolvent, and liquid-assisted grinding) demonstrated the co-crystal's consistent morphological integrity, an essential factor for scalable production. Furthermore, the dissolution studies of the co-crystal, especially in tablet form, are of significant interest. The enhanced dissolution rates observed for the PROG-PABA co-crystal compared to pure PROG suggest improved bioavailability, a key consideration in oral drug delivery. The study's findings here are in line with the current trend in pharmaceutical research focusing on improving drug dissolution rates, as this directly impacts the drug's therapeutic efficacy. The superior dissolution rate of the tablet form compared to existing formulations demonstrates the potential of this co-crystal in enhancing drug delivery efficiency. This part of the study is particularly relevant in the context of the ongoing search for more effective oral pharmaceutical formulations.

5. Conclusions

A new co-crystal of PROG and PABA with distinct physical properties is reported and successfully produced through solution crystallisation and liquid assisted grinding methods. PROG-PABA crystal structure was solved through SC-XRD and distinct crystalline melting point reported using DSC. Of the three scale up methods trialled, liquid assisted grinding was selected as the most suitable for PROG-PABA preparation since spray drying and antisolvent methods were observed to form a mixture of co-crystal and starting material phases. When assessing physical properties, PROG-PABA co-crystal showed distinct solubility and more complete dissolution in aqueous media than PROG starting material. Following formulation into tablets, the PROG-PABA co-crystal showed a significant increase in the % dissolution compared to the Utrogestan® soft-gel capsule formulation. The marked increase in dissolution for the co-crystal tablet formulation may help increase the oral bioavailability for PROG through a cost-efficient alternative to the current formulation. Further studies to optimise the spray drying and antisolvent production methods as a rapid option for co-crystal preparation are required.

CRediT authorship contribution statement

Thomas Hibbard: Conceptualization, Investigation, Methodology, Writing – original draft, Writing – review & editing. **Kenneth Shankland:** Conceptualization, Investigation, Writing – original draft, Writing – review & editing. **Hisham Al-Obaidi:** Conceptualization, Investigation, Methodology, Supervision, Writing – original draft, Writing – review & editing.

Declaration of competing interest

The authors declare that they have no known competing financial interests or personal relationships that could have appeared to influence the work reported in this paper.

Data availability

Data will be made available on request.

Appendix A. Supplementary material

Supplementary data to this article can be found online at https://doi.org/10.1016/j.ejpb.2024.114202.

References

[1] N. Asi, K. Mohammed, Q. Haydour, M.R. Gionfriddo, O.L. Vargas, L.J. Prokop, S. S. Faubion, M.H. Murad, Progesterone vs. synthetic progestins and the risk of breast cancer: a systematic review and meta-analysis, Syst. Rev. 5 (2016) 121.
[2] S. Furness, H. Roberts, J. Marjoribanks, A. Lethaby, Hormone therapy in postmenopausal women and risk of endometrial hyperplasia, Cochrane Database Syst. Rev. 2012 (2012) CD000402.
[3] G.N. Wagh, K.M. Kundavi Shankar, S. Bachani, A review of conventional and sustained-release formulations of oral natural micronized progesterone in obstetric indications, Drugs Context 10 (2021).
[4] F. Damian, M. Harati, J. Schwartzenhauer, O. Van Cauwenberghe, S.D. Wettig, Challenges of dissolution methods development for soft gelatin capsules, Pharmaceutics 13 (2021) 214.
[5] H. Al-Obaidi, M. Majumder, F. Bari, Amorphous and crystalline particulates: challenges and perspectives in drug delivery, Curr. Pharm. Des. 23 (2017) 350–361.
[6] T. Hibbard, B. Nyambura, P. Scholes, M. Totolici, K. Shankland, H. Al-Obaidi, Preparation and physiochemical analysis of novel ciprofloxacin/dicarboxylic acid salts, J. Pharm. Sci. 112 (2023) 195–203.
[7] J.F. Remenar, S.L. Morissette, M.L. Peterson, B. Moulton, J.M. MacPhee, H. R. Guzman, O. Almarsson, Crystal engineering of novel cocrystals of a triazole drug with 1,4-dicarboxylic acids, J. Am. Chem. Soc. 125 (2003) 8456–8457.
[8] M. Samipillai, S. Rohani, The role of higher coformer stoichiometry ratio in pharmaceutical cocrystals for improving their solid-state properties: the cocrystals of progesterone and 4-hydroxybenzoic acid, J. Cryst. Growth 507 (2019) 270–282.
[9] C. Guo, Q. Zhang, B. Zhu, Z. Zhang, X. Ma, W. Dai, X. Gong, G. Ren, X. Mei, Drug–drug cocrystals provide significant improvements of drug properties in treatment with progesterone, Cryst. Growth Des. 20 (2020) 3053–3063.
[10] H. Zeng, J. Xiong, Z. Zhao, J. Qiao, D. Xu, M. Miao, L. He, X. Wu, Preparation of progesterone co-crystals based on crystal engineering strategies, Molecules 24 (2019) 3936.
[11] Y. Yunxia, N. Huihui, X. Shiying, G. Yingwa, W. Xiangxiang, Solubility and dissolution rate of progesterone cocrystals using 4-fluorobenzoic acid and 2-hydroxy-6-naphthoic acid as coformers, J. Cryst. Growth 585 (2022) 126601.
[12] H. Zeng, J. Xiong, Z. Zhao, J. Qiao, D. Xu, M. Miao, L. He, X. Wu, Preparation of progesterone co-crystals based on crystal engineering strategies, Molecules 24 (2019).
[13] B.J. Boyd, C.A.S. Bergstrom, Z. Vinarov, M. Kuentz, J. Brouwers, P. Augustijns, M. Brandl, A. Bernkop-Schnurch, N. Shrestha, V. Preat, A. Mullertz, A. Bauer-Brandl, V. Jannin, Successful oral delivery of poorly water-soluble drugs both depends on the intraluminal behavior of drugs and of appropriate advanced drug delivery systems, Eur. J. Pharm. Sci. 137 (2019) 104967.
[14] C.L. Vo, C. Park, B.J. Lee, Current trends and future perspectives of solid dispersions containing poorly water-soluble drugs, Eur. J. Pharm. Biopharm. 85 (2013) 799–813.
[15] M. Karimi-Jafari, L. Padrela, G.M. Walker, D.M. Croker, Creating cocrystals: a review of pharmaceutical cocrystal preparation routes and applications, Cryst. Growth Des. 18 (2018) 6370–6387.
[16] L. Fábián, Cambridge structural database analysis of molecular complementarity in cocrystals, Cryst. Growth Des. 9 (2009) 1436–1443.
[17] P. Ying, J. Yu, W. Su, Liquid-assisted grinding mechanochemistry in the synthesis of pharmaceuticals, Adv. Synth. Catal. 363 (2021) 1246–1271.
[18] G.M. Sheldrick, SHELXT–Integrated space-group and crystal-structure determination, Acta Crystallogr. Sect. A: Found. Adv. 71 (2015) 3–8.
[19] G.M. Sheldrick, Crystal structure refinement with SHELXL, Acta Crystallogr. Sect. C: Struct. Chem. 71 (2015) 3–8.
[20] O.V. Dolomanov, L.J. Bourhis, R.J. Gildea, J.A. Howard, H. Puschmann, OLEX2: a complete structure solution, refinement and analysis program, J. Appl. Cryst. 42 (2009) 339–341.
[21] C.R. Groom, I.J. Bruno, M.P. Lightfoot, S.C. Ward, The Cambridge structural database, Acta Crystallogr. Sect. B: Struct. Sci. Cryst. Eng. Mater. 72 (2016) 171–179.
[22] C.F. Macrae, I. Sovago, S.J. Cottrell, P.T. Galek, P. McCabe, E. Pidcock, M. Platings, G.P. Shields, J.S. Stevens, M. Towler, Mercury 4.0: from visualization to analysis, design and prediction, J. Appl. Cryst. 53 (2020) 226–235.

[23] A. Sarkar, D. Ragab, S. Rohani, Polymorphism of progesterone: a new approach for the formation of form II and the relative stabilities of form I and form II, Cryst. Growth Des. 14 (2014) 4574–4582.
[24] MHRA, British pharmacopoeia, Medicines and Healthcare Products Regulatory Agency, 2023, pp. Appendix XII C. Consistency of Formulated Preparations.
[25] B. Mittal, How to Develop Robust Solid Oral Dosage Forms: From Conception to Post-approval, Academic Press, 2016.
[26] B.A. Bernick, J.M. Amadio, P.H. Persicaner, J.L. Cacace, T. Thorsteinsson, F.D. Sancilio, Progesterone formulations, Google Patents, 2018.
[27] B. Agnus, A. Besins, Progesterone tablet and its manufacturing process, Google Patents, 2000.
[28] D.D. Bavishi, C.H. Borkhataria, Spring and parachute: How cocrystals enhance solubility, Prog. Cryst. Growth Charact. Mater. 62 (2016) 1–8.